Contribution from the Department of Chemistry,
Northeastern University, Boston, Massachusetts 02115

Thiocyanate-Bridged Transition-Metal Polymers. 2. Investigation of a Structural Phase Transition in Polymeric (Bipyridyl)iron(II) Thiocyanate, $Fe(bpy)(NCS)_2$

BRUCE W. DOCKUM and WILLIAM MICHAEL REIFF*

Received July 30, 1981

$Fe(bpy)(NCS)_2$ has been shown to undergo a reversible structural phase transition between 130 and 185 K with use of Mössbauer spectroscopy. Additional characterization using differential scanning calorimetry, optical spectroscopy, and cryomagnetic susceptibility measurements is also discussed.

Introduction

We have previously reported the structural, electronic, and magnetic properties of $Fe(bpy)(NSC)_2$ using a variety of experimental techniques.[1] This compound is prepared by vacuum thermolysis of $Fe(bpy)_2(NCS)_2$ at ca. 200 °C and is obtained as a very finely divided powdery material that gives broadened lines in its X-ray powder pattern. From this study, we proposed that $Fe(bpy)(NCS)_2$ is a polymer whose structure consists of stepwise, zigzag chains containing six-coordinate iron centers bridged by thiocyanate anions (Figure 1). Magnetic measurements to 1.6 K indicate antiferromagnetic exchange interactions within the polymer chains.

$Fe(bpy)(NCS)_2$ exhibits interesting Mössbauer behavior as a function of temperature.[1] At room temperature, the spectrum shows a single, narrow quadrupole doublet (ΔE_Q = 0.397 mm/s). When $Fe(bpy)(NCS)_2$ is cooled to ~110 K, a single quadrupole doublet is also observed, but it has a considerably greater magnitude (ΔE_Q = 2.579 mm/s). At ~155 K, *two quadrupole doublets*, an inner doublet corresponding to the doublet at higher temperatures and an outer doublet corresponding to that found at lower temperatures, are observed. The isomer shift for each doublet is near 1.0 mm/s. These results suggest that $Fe(bpy)(NCS)_2$ undergoes *a structural phase transformation* as the temperature is decreased. This behavior is in contrast to that observed for the extensively investigated precursor bis(bipyridyl) compound $Fe(bpy)_2(NCS)_2$, which is known to undergo a reversible ground-state spin multiplicity change: $^1A_{1g} \rightleftarrows {}^5T_{2g}$.[2] The spin-state change in $Fe(bpy)_2(NCS)_2$ does not involve space-group or lattice parameter changes but is accompanied by the expected shortening of the Fe–N(NCS) and Fe–N(bpy) bond lengths when the $^1A_{1g}$ ground state is populated.[3] During the spin-state change, the Mössbauer spectrum of $Fe(bpy)_2(NCS)_2$, which exhibits a large quadrupole splitting at room temperature, is transformed into a smaller doublet with a corresponding expected *large decrease* in *the isomer shift*, the latter being consistent with the decrease in spin multiplicity.[2] The phase transition observed for $Fe(bpy)(NCS)_2$ that we now consider in greater detail is thought to involve a displacive realignment of the entire polymer chain originating from a change in the symmetry of the metal–bridging ligand framework. This type of phase change has been observed in a detailed single-crystal study of $Co(py)_2Cl_2$[4,5] and in the iron,[6-8] manganese,[9] and nickel[9] bis(pyridyl) chlorides as well as $Co(py)_2Cl_2$[7] by Mössbauer transmission and emission measurements.

Table I. Mössbauer Parameters for the High- and Low-Temperature Phases of $Fe(bpy)(NCS)_2$

phase	T, K	$\delta^{a,b}$	$\Delta E_Q{}^a$	$\Gamma_1{}^{a,c}$	$\Gamma_2{}^{a,c}$	$\Gamma_1/\Gamma_2{}^c$	$A_1/A_2{}^c$
LT	1.57	1.121	2.955	0.377	0.407	0.926	1.016
	4.2	1.124	2.934	0.324	0.326	0.994	1.016
	20.01	1.123	2.931	0.343	0.336	1.022	1.026
	41.51	1.120	2.925	0.307	0.305	1.006	1.037
	69.97	1.114	2.869	0.308	0.306	1.006	1.006
	110.12	1.104	2.579	0.358	0.345	1.038	1.048
	120.16	1.100	2.413	0.406	0.395	1.028	1.018
	130.28	1.094	2.179	0.492	0.501	0.982	1.002
HT	212.10	1.046	0.542	0.485	0.442	1.097	1.165
	300	0.949	0.394	0.299	0.296	1.010	1.057

[a] These quantities are expressed in mm/s. [b] Relative to iron foil at 300 K. [c] Subscript 1 refers to the peak at lower velocities; subscript 2 refers to the peak at higher velocities.

Experimental Section

$Fe(bpy)(NCS)_2$ is a new compound and was prepared by a method reported earlier.[1] The compound gave a satisfactory elemental analysis. Anal. Calcd: C, 43.92; H, 2.46; N, 17.12. Found: C, 43.68; H, 2.45; N, 16.93. The Mössbauer spectra were taken with a spectrometer and low-temperature equipment previously described.[10,11] The Mössbauer spectra were fit to a sum of Lorentzian lines with use of a modified version of the program of Stone.[12] Differential scanning calorimetry (DSC) measurements were performed with a Perkin-Elmer Model DSC-1B calorimeter and a Du Pont 990 thermal analyzer.

Results and Discussion

Mössbauer Spectroscopy. The Mössbauer spectra for $Fe(bpy)(NCS)_2$ measured between room temperature and 110 K indicate that the phase transformation occurs between 130 and 185 K. Figures 2 and 3 show the spectra in the latter temperature range. The parameters obtained from Lorentzian fitting are given in Tables I and II corresponding to single- and two-phase temperature regions, respectively. The spectra consist of two broadened quadrupole doublets in which the inner doublet corresponds to the contribution of the high-temperature (HT) phase while the outer doublet corresponds to the low-temperature (LT) phase. The isomer shift (δ) for *each phase* is ~1.0 mm/s. Thus, the phase transformation *does not involve a change of spin multiplicity* from the ground spin quintet of high-spin ferrous ion. A Mössbauer spectrum was also determined at 77 K with both the source and the absorber at the same temperature, and the isomer shift was the same as that observed at 300 K. This indicates that the

(1) Part 1: B. W. Dockum and W. M. Reiff, Abstracts, 2nd Joint Conference of the Chemical Institute of Canada and the American Chemical Society, Montreal, Canada, May 1977, No. INOR 9; *Inorg. Chem.*, **21**, 391 (1982).
(2) E. König, K. Madeja, and K. J. Watson, *J. Am. Chem. Soc.*, **90**, 1146 (1968).
(3) E. König and K. J. Watson, *Chem. Phys. Lett.*, **6**, 457 (1970).
(4) P. J. Clarke and H. J. Milledge, *Acta Crystallogr., Sect. B*, **B31**, 1543 (1975).
(5) P. J. Clarke and H. J. Milledge, *Acta Crystallogr., Sect. B*, **B31**, 1554 (1975).
(6) G. J. Long, D. L. Whitney, and J. E. Kennedy, *Inorg. Chem.*, **10**, 1406 (1971).
(7) J. P. Sanchez, L. Asch, and J. M. Friedt, *Chem. Phys. Lett.*, **18**, 250 (1973).
(8) W. M. Reiff, R. B. Frankel, B. F. Little, and G. J. Long, *Chem. Phys. Lett.*, **28**, 68 (1974).
(9) T. Yoshihashi and H. Sano, *Chem. Phys. Lett.*, **34**, 289 (1975).
(10) W. M. Reiff and C. Cheng, *Inorg. Chem.*, **16**, 2097 (1977).
(11) C. Cheng, H. Wong, and W. M. Reiff, *Inorg. Chem.*, **16**, 819 (1977).
(12) G. M. Bancroft, A. G. Maddock, W. K. Ong, R. H. Prince, and A. J. Stone, *J. Chem. Soc. A*, 1966 (1967).

0020-1669/82/1321-1406$01.25/0

Table II. Mössbauer Parameters[a] for Fe(bpy)(NCS)$_2$ in the Temperature Range of the Phase Transition

	line widths[b,d]						areas[d]					
T, K	Γ_1 (LT)	Γ_2 (HT)	Γ_3 (HT)	Γ_4 (LT)	Γ_1/Γ_4 (LT)	Γ_2/Γ_3 (HT)	A_1(LT)	A_2(HT)	A_3(HT)	A_4(LT)	A_1/A_4 (LT)	A_2/A_3 (HT)
140.08	0.671	0.580	0.817	0.496	1.353	0.709	485 986	96 705	325 104	225 055	2.159	0.297
145.10	0.655	0.684	0.788	0.582	1.125	0.868	413 764	16 785	256 306	308 423	1.342	0.654
150.16	0.797	0.320	0.444	0.800	0.996	0.720	653 914	99 710	136 481	576 428	1.134	0.730
155.15	0.760	0.480	0.505	0.721	1.054	0.950	512 529	157 224	173 790	445 863	1.124	0.904
160.24	0.774	0.355	0.494	0.653	1.185	0.718	425 332	114 861	197 717	312 266	1.362	0.580
165.27	0.915	0.302	0.271	0.831	1.101	1.114	459 936	127 495	106 213	403 607	1.140	1.200
169.86	0.822	0.350	0.270	0.846	0.971	1.296	326 709	168 212	118 752	353 323	0.924	1.416
185.34	0.802	0.272	0.237	0.616	1.302	1.148	260 803	113 237	92 498	212 629	1.227	0.435

T, K	$\delta(1-4)^{b,c}$ (LT)	$\delta(2-3)^{b,c}$ (HT)	ΔE_Q (2-3)[b] (LT)	ΔE_Q (2-3)[b] (HT)	χ^2	T, K	$\delta(1-4)^{b,c}$ (LT)	$\delta(2-3)^{b,c}$ (HT)	ΔE_Q (2-3)[b] (LT)	ΔE_Q (2-3)[b] (HT)	χ^2
140.08	1.118	1.194	1.945	1.127	178.88	160.24	1.101	1.090	1.662	0.694	207.35
145.10	1.098	1.106	1.928	1.054	188.19	165.27	1.064	1.068	1.275	0.554	191.14
150.16	1.082	1.090	1.641	0.667	206.00	169.86	1.038	1.068	1.294	0.579	193.49
155.15	1.069	1.068	1.671	0.726	209.88	185.34	1.049	1.055	0.940	0.496	207.64

[a] Source at ambient temperature. [b] These quantities are expressed in mm/s. [c] Relative to iron foil at 300 K. [d] Subscripts 1-4 for line widths, areas, δ's and ΔE_Q's refer to order of peaks in a spectrum. Subscript 1 refers to the peak lowest in energy and 4 to the peak highest in energy.

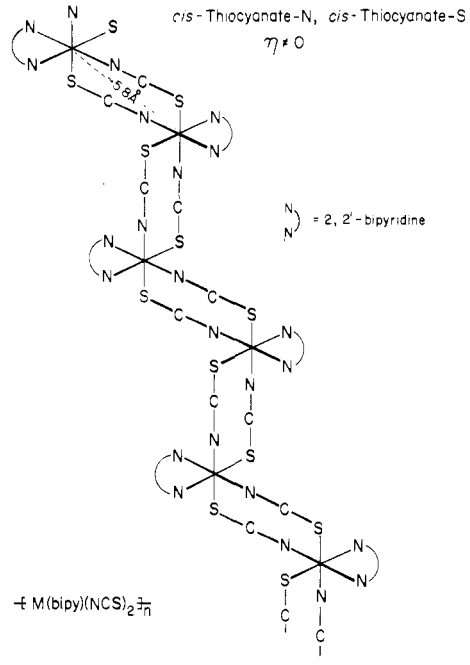

Figure 1. Proposed structure of Fe(bpy)(NCS)$_2$.

phase transformation is *not accompanied* by a change of metal ion coordination number. The value of $\delta \approx 1$ mm/s is fully consistent with pseudooctahedral coordination, i.e., six-coordinate iron(II) in a covalently bound $FeN_2N'_2S_2$ chromophore.

There is an increase in the quadrupole splitting for each phase with decreasing temperature, indicating a gradual depopulation of the excited iron electronic states. As the temperature decreases, the contribution of the HT phase gradually diminishes as can be observed by the increasing contribution of the quadrupole doublet of the LT phase to the composite curve obtained from the Lorentzian fits. Below 130 K, the HT phase has essentially vanished. In the temperature range ~145 to ~160 K, the contributions made by each phase are clearly evident in the raw data. If the temperature is varied up or down through the phase transition, there is little, if any, hysteresis observed. Determination of Mössbauer spectra with careful temperature equilibration for either increasing or decreasing temperature sequences clearly shows the reversibility of the transition. Above and below these temperatures, the spectral peaks are so highly overlapped that peak asymmetry and non-Lorentzian line shapes are seen as opposed to four distinct transitions. The areas of the individual peaks in the quadrupole doublet of each phase are generally unequal, indicating the possibility of texture and/or Goldanskii–Karyagin asymmetry. We have, however, made no attempt at detailed analysis of the spectra from the point of view of the foregoing effects owing to difficulty in obtaining *unique fits* for such highly overlapped spectral patterns. The total area of the peaks in the quadrupole doublet of the LT phase is always greater than those for the HT phase at each temperature measured. These results indicate a greater Debye–Waller factor, or recoil-free fraction, for the LT phase of Fe(bpy)(NCS)$_2$. Large, discontinuous increases in the recoil-free fraction have been observed in the Mössbauer study of the phase transitions of systems containing the $Fe(NH_3)_6^{2+}$ cation as such compounds are cooled through their transition temperature, forming a more crystallographically distorted phase.[13] Also, in Mössbauer studies of the *displacive* phase transitions of α-Fe(py)$_2$Cl$_2$ and α-Co(py)$_2$Cl$_2$, chain polymers more relevant to the present study, a similar sharp variation in the area ratio of the quadrupole doublets at the transition temperature was observed, indicating a difference in the Debye–Waller factors of each phase.[7]

Spectral and Cryomagnetic Studies. In addition to the foregoing Mössbauer studies, we have measured the near-infrared–visible and infrared spectra at low temperatures in a search for additional evidence and characterization of the phase transition involved. Neither the optical spectra in the range 5000–20 000 cm^{-1} nor the infrared spectra in the carbon–nitrogen stretching region (2000–2150 cm^{-1}) exhibited significant changes on cooling to 77 K. This includes visual inspection of samples as they were cooled. This is perhaps not unexpected in view of the low symmetry of the chromophore involved (Figure 1). On the other hand, there is clear evidence of two magnetic species and the phase transformation in the temperature dependence of the reciprocal molar susceptibility shown in Figures 4 and 5. These data are the result of vibrating-sample magnetometry measurements at a large number (>130) of temperatures. The curvature and non-Curie–Weiss law behavior above ca. 80 K are obvious. The minimum in χ_g^{-1} at ~20 K corresponds to the maximum in χ_M' (Figure 5) and has been discussed previously. In the ranges 40–110 and 170–300 K, it is possible to fit χ_g^{-1} vs. T

(13) L. Asch, G. K. Shenoy, J. M. Friedt, J. P. Adloff, and R. Kleinberger, *J. Chem. Phys.*, **62**, 2335 (1975).

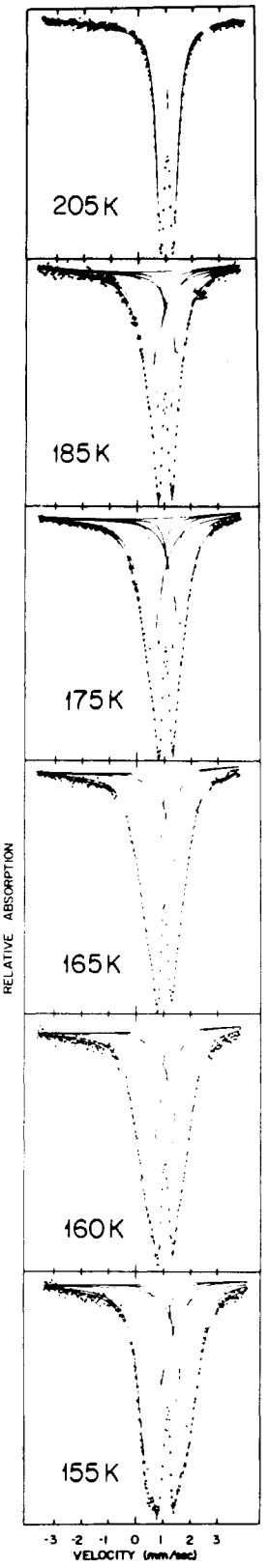

Figure 2. Mössbauer spectra including Lorentzian fits taken in the *decreasing* temperature range 205–155 K.

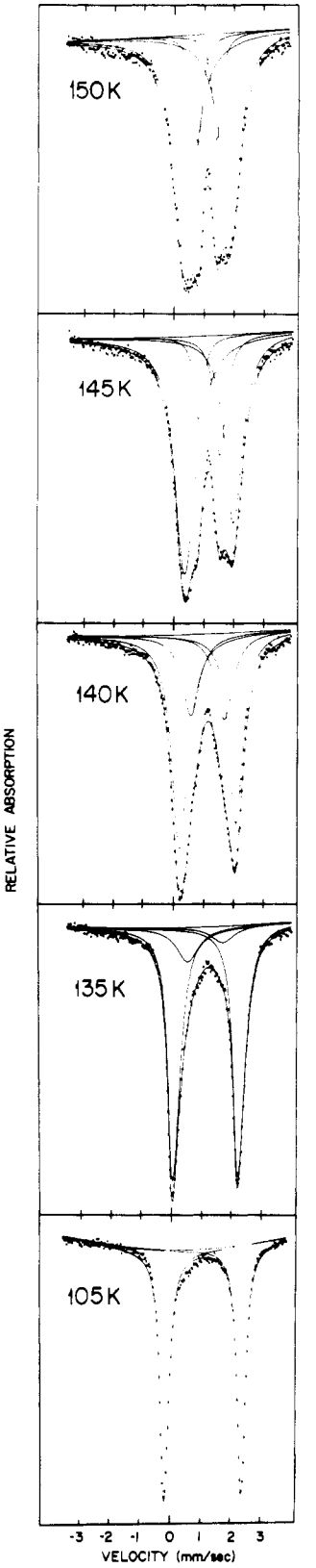

Figure 3. Mössbauer spectra including Lorentzian fits taken in the *decreasing* temperature range 150–105 K.

with two Curie–Weiss laws with the former range corresponding to a positive paramagnetic Curie temperature (Θ) $\sim$+20 K and the latter corresponding to $\Theta \approx -35$ K. A more dramatic method of viewing the magnetic data (and that indicates the onset of the phase transition above ca. 100 K) is our attempt to least-squares fit χ_M' vs. T to a single antiferromagnetic exchange parameter, J. We are able to obtain reasonable fits to the low-temperature susceptibility data for parameters as given in Figure 5 up to $\sim$100 K, above which (in the two-phase region) the fit begins to show progressive deviation.

Nature of the Phase Transition. As mentioned in the Introduction, we assume that the structural phase transformation is roughly similar in nature to the $\alpha \rightarrow \gamma$ transition observed for the linear-chain $M(py)_2Cl_2$ systems, at 234 K for M = Fe and 150 K for M = Co. The latter involves a polymer chain

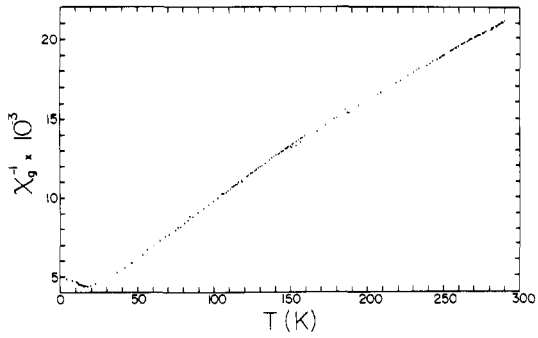

Figure 4. Reciprocal gram-susceptibility ($\chi_g'^{-1}$) vs. temperature over the range 300–2.0 K.

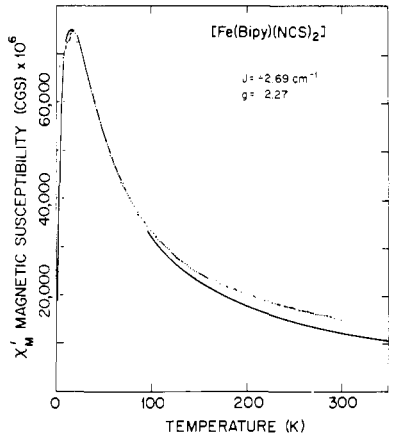

Figure 5. Molar susceptibility and superimposed least-squares fit for weak antiferromagnetic exchange over the range 300–2 K using the Heisenberg–Dirac–Van Vleck dipolar coupling model as discussed in ref 1 (part 1 of this series).

displacement from the high-temperature symmetrically chloro-bridged α form to the asymmetric γ form:

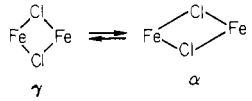

γ α

(the β form of $Co(py)_2Cl_2$ is a pseudotetrahedral *monomer*). In view of the fact that we do not as yet have X-ray structure data for any form of $Fe(bpy)(NCS)_2$, the following is clearly speculative. However, we have recently[14] determined the molecular structure of the related $Co(bpy)Cl_2$ (Figures 6 and 7). The adjacent chains of this zigzag polymer are interleaved with interchain overlap of the bipyridine rings by ~20% of their areas. There is similar interleaving overlap for α- and γ-$Co(py)_2Cl_2$. Thus, we tentatively propose that observed Mössbauer spectroscopy and magnetic behavior of $Fe(bpy)(NCS)_2$ correspond to an analogous reversible α to γ type transition involving distortion of the NCS bridging framework and probable sliding of overlapping aromatic rings past each other. The primary distortion of the bridging framework most likely involves changes in the MSC angles, there being less flexibility to carbon–nitrogen double bonds.

The large temperature interval (~50 K) over which the phase transition occurs as measured by Mössbauer spectroscopy may be indicative of a second-order phase transition, i.e., a gradual change without a characteristic latent heat. In contrast, an ideal first-order phase transition usually occurs more suddenly with an entropy discontinuity and associated latent heat. However, a first-order phase transition may be

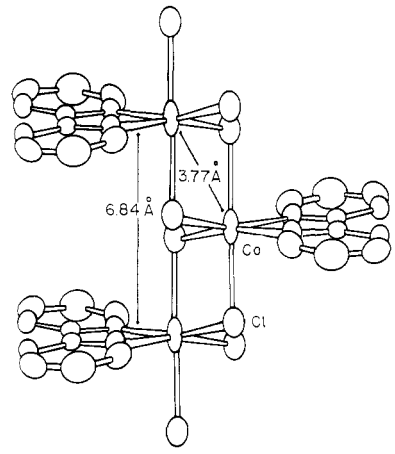

Figure 6. Local bridging framework in polymeric $Co(bpy)Cl_2$.

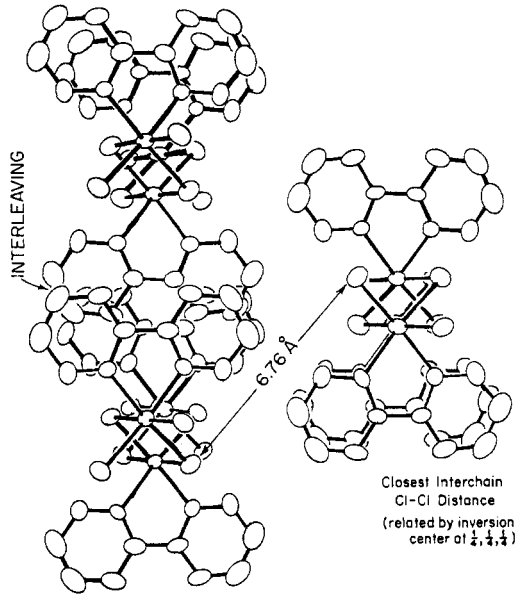

Figure 7. Packing diagram showing chain interleaving in $Co(bpy)Cl_2$.

disguised as a second-order transition if a system has a large number of "defects" in the crystal lattice. The method of preparation for $Fe(bpy)(NCS)_2$ can very easily introduce these defects into the lattice, in particular, broken metal–thiocyanate bridge bonds. Such defects can increase the temperature interval over which the transition occurs and may also be the reason for the broadened peaks observed in the Mössbauer spectra. This prevents a detailed analysis of the areas as presented by the method of Lang.[15-17] The effects of the introduction of lattice defects have been demonstrated in a recent Mössbauer spectroscopic study of the perovskite-type layer compound $(CH_3NH_3)_2FeCl_4$.[18] When it was freshly prepared as a polycrystalline, nonpulverized powder, one of its layer "tilting" phase transitions was readily observed. The same transition was no longer observed when the sample was pulverized. It is quite likely that the phase transition for $Fe(bpy)(NCS)_2$ is, in fact, a first-order transition as found in the $\alpha \rightarrow \gamma$ transition in $Co(py)_2Cl_2$ or the isomorphous $Fe(py)_2Cl_2$. A differential scanning calorimetry (DSC) study of $Fe(bpy)(NCS)_2$ between 125 and 300 K did not reveal well-defined endotherms (with increasing T) or exotherms

(14) G. A. Eisman, H. Wong, W. M. Reiff, W. Rode, and B. Foxman, Abstracts, 179th National Meeting of the American Chemical Society, Houston, TX, March 1980, No. INOR 22.

(15) G. Lang, *Nucl. Instrum. Methods*, **24**, 425 (1963).
(16) E. König, G. Ritter, *Mössbauer Eff. Methodol.*, **9**, 3 (1974).
(17) E. König, G. Ritter, W. Irler, and S. M. Nelson, *Inorg. Chim. Acta*, **37**, 169 (1979).
(18) C. Nicolini and W. M. Reiff, *J. Phys., Colloq. (Orsay, Fr.)*, **41**, 1-295 (1980).

(with decreasing T) associated with a first-order transition. In a differential scanning calorimetry study of the $\gamma \rightarrow \alpha$ transition of the manganese, iron, and cobalt bis(pyridyl) chloride compounds ($M(py)_2Cl_2$), we have observed endotherms for crystalline-solution preparations.[19] A final conclusion concerning the thermodynamic order of the transition must await further study. Solution preparations of a more crystalline, less defect-containing form of $Fe(bpy)(NCS)_2$ may be helpful in this regard and are being attempted.

Acknowledgment. The authors wish to acknowledge the support of the National Science Foundation, Division of Materials Research, Solid State Chemistry Program (Grant No. DMR-80-16441), and the assistance of G. A. Eisman in obtaining low-temperature differential scanning calorimetry data.

Registry No. $Fe(bpy)(NCS)_2$, 79803-24-0.

(19) G. A. Eisman and W. M. Reiff, *Inorg. Chim. Acta*, **44**, L171 (1980).

Contribution from the Department of Chemistry, University of Oklahoma, Norman, Oklahoma 73019

Oxy and Thio Phosphorus Acid Derivatives of Tin. 8. Tin(II) Bis(dithiophosphate) Esters and Their Bipyridyl Adducts. X-ray Crystal and Molecular Structure of Bis(*O*,*O*′-diphenyl dithiophosphato)tin(II), a Bicyclic Dimer Held Together by Three-Coordinated Sulfur Atoms and by η^6-C_6H_5 Interactions Binding Tin(II) Lone Pairs to Phenoxy Ester Groups[1-3]

J. L. LEFFERTS, K. C. MOLLOY, M. B. HOSSAIN, D. VAN DER HELM, and J. J. ZUCKERMAN*[4]

Received June 1, 1981

Four tin(II) dithiophosphate esters, $Sn[S_2P(OR)_2]_2$, where R = CH_3, C_2H_5, i-C_3H_7, or C_6H_5, are synthesized in high yield by the action of the *O*,*O*′-diorganodithiophosphoric acids on dimethoxytin(II) in benzene to release methanol. The R = C_2H_5 product is a pale yellow oil, but the others are colorless crystalline solids soluble in nonpolar organic solvents. The 2,2′-bipyridyl adducts of the parent esters form immediately upon mixing. NMR coupling is observed from the ester groups to phosphorus, as $|^3J(^{31}P\text{-}O\text{-}C\text{-}^1H)|$ = 15.5 Hz in the R = CH_3 derivative. Infrared spectral assignments can be made for the $\nu_{asym}(PS_2)$ (660–627 cm^{-1}), $\nu_{sym}(PS_2)$ (525–505 cm^{-1}), ν[(P)O–C] (1190–1150 cm^{-1}), ν[P–O(C)] (1030–1010 cm^{-1}), and ν(SnS) (355–332 cm^{-1}) modes. In the mass spectra parent molecular ions are found for all the species, but the fragments resulting from the loss of one ligand moiety are more abundant. The chief pathway for the decomposition is the successive loss of ligand moieties. Ditin-bearing ions are detected in the spectrum of the R = C_2H_5 derivative. The mass spectra of the bipyridyl adducts are the superposition of those of the parent tin(II) esters and of bipyridyl. The tin-119m Mössbauer isomer shifts (IS = 3.66–3.78 mm s^{-1}) confirm the presence of tin(II), and the barely resolvable quadrupole splittings (QS = 0.97–1.06 mm s^{-1}) do not increase on complexation by bipyridyl (1.03–1.15 mm s^{-1}), suggesting that the parent tin(II) esters themselves have higher coordination number in the solid state. Bis(*O*,*O*′-diphenyl dithiophosphato)tin(II), $C_{24}H_{20}O_4S_4P_2Sn$, crystallizes in the triclinic space group $P\bar{1}$ with a = 10.499 (5) Å, b = 13.948 (7) Å, c = 9.291 (4) Å, α = 99.18 (6)°, β = 95.71 (5)°, and γ = 91.80 (5)°, at 138 ± 2 K. The structure was determined by Patterson and Fourier techniques from 5517 reflections measured at 138 ± 2 K on an automatic diffractometer with monochromatic Mo Kα radiation and refined to a final R value of 0.029 for all data. The centrosymmetric dimer contains one ligand bridging two tin atoms intermolecularly, while simultaneously chelating one tin atom in an extremely anisobidentate fashion via a bifurcated, three-coordinated sulfur atom [S(4)]. A second ligand is involved in normal chelation. Completing the coordination sphere at the tin(II) atom and contributing to the formation of the dimer is an η^6-C_6H_5 interaction between the phenoxy ester group of the bridging ligand of the second molecular unit and the tin(II) lone pair to produce a ψ-6-coordinated metal center. A planar Sn_2S_2 ring is demanded by crystallographic symmetry and is seen to be circumscribed by an eight-membered $[SnSPS]_2$ ring in a chair conformation. The ester P(1)—S(1)—Sn(1) and P(2)—S(3)—Sn(1) systems are distinguished from the double-bonded, dative P(1)=S(2)→Sn(1), P(2)=S(4)→Sn(1), and P(2′)=S(4′)→Sn(1) systems on the basis of their P—S and S—Sn internuclear distances. The tin atom is 0.46 Å out of the plane formed by the S(1), S(2), S(4), and S(4′) atoms and is away from the S(3) atom, with the ester-bound sulfur atoms cis oriented [∠S(1)–Sn(1)–S(3) = 87.41°]. The smallest angle in the plane is formed by the terminally chelating sulfur atoms [∠S(1)–Sn(1)–S(2) = 74.28°]. Atom S(3) is opposite the expected direction of the tin(II)-lone-pair vector, which if extended strikes a perpendicularly oriented phenoxy group with tin to carbon distances at 3.457–4.317 Å. The distances to the center of the ring and to the plane of the ring are 3.66 and 3.46 Å, respectively. The ordering of the angles at the phosphorus atoms obeys the expected isovalent hybridization predictions: ∠S–P–S > ∠S–P–O > ∠O–P–O. The stability of the phenoxy ester to air oxidation is rationalized in terms of the additional η^6-C_6H_5 bonding contribution and by the steric blocking of the tin(II) lone pair by the phenoxy group.

In this series of papers we have been studying the synthetic routes to organotin(IV) derivatives of various oxy and thio phosphorus acids, and the spectroscopic properties and structures of the resulting products.[1] We have also had an interest in tin(II) chemistry extending over 20 years.[5] This paper is the issue of the marriage of these two themes. We report the synthesis of four tin(II) dithiophosphate esters, their adducts with 2,2′-bipyridyl, and the remarkable and unexpected crystal structure of the diphenyl ester derivative.

(1) For part 7 of this series see: Molloy, K. C.; Hossain, M. B.; van der Helm, D.; Cunningham, D.; Zuckerman, J. J. *Inorg. Chem.* **1981**, *20*, 2402.
(2) The crystal structure of bis(*O*,*O*′-diphenyl dithiophosphato)tin(II) has been published in a preliminary form.[3]
(3) Lefferts, J. L.; Hossain, M. B.; Molloy, K. C.; van der Helm, D.; Zuckerman, J. J. *Angew. Chem., Int. Ed. Engl.* **1980**, *19*, 309.
(4) To whom correspondence should be addressed.
(5) Zuckerman, J. J. *J. Chem. Soc.* **1963**, 1322.

0020-1669/82/1321-1410$01.25/0